Diamond & Related Materials 101 (2020) 107624

Contents lists available at ScienceDirect

Diamond & Related Materials

journal homepage: www.elsevier.com/locate/diamond

# Effect of voltage applied for graphene oxide/latex nanocomposites produced via electrochemical exfoliation and its application as conductive electrodes

M.D. Nurhafizah[a,*], A.B. Suriani[b,c], A. Mohamed[c,d], T. Soga[e]

[a] Nano-Optoelectronics Research and Technology Laboratory, School of Physics, Universiti Sains Malaysia, 11800 Minden Penang, Malaysia
[b] Department of Physics, Faculty of Science and Mathematics, Universiti Pendidikan Sultan Idris, 35900 Tanjung Malim, Perak, Malaysia
[c] Nanotechnology Research Centre, Faculty of Science and Mathematics, Universiti Pendidikan Sultan Idris, 35900 Tanjung Malim, Perak, Malaysia
[d] Department of Chemistry, Faculty of Science and Mathematics, Universiti Pendidikan Sultan Idris, 35900 Tanjung Malim, Perak, Malaysia
[e] Department of Frontier Materials, Nagoya Institute of Technology, Gokiso-cho, Showa-ku, Nagoya 466-8555, Japan

ARTICLE INFO

*Keywords:*
Composites
Oxidation
Surface characterization
Electrical conductivity
Electrodes

ABSTRACT

An electrochemical exfoliation method adopted in this study presents the variations quality of GO produced under different applied voltages. The GOs production was characterized using FESEM, AFM, micro-Raman, FT-IR, and UV–Vis spectroscopies. Further characterizations were done using I-V, C-V, mechanical, and TGA analysis. As evident, GOs at 10 V shows the highest quality and several thin GO layers produced with moderate crystallinity of 0.91. In this study, GOs filled in the nanocomposites synthesized at 5 to 10 V shows higher electrical conductivity and acceptable capacitance performance at approximate $\sim\times10^{-5}$ to $\times10^{-7}$ S cm$^{-1}$ and up to 2.5–103 F g$^{-1}$, respectively. These thin films paved the way and great potential to be implemented as flexible electrodes materials in supercapacitor application.

## 1. Introduction

In recent years, the Graphene Oxide (GO) production via green solution-based processing namely electrochemical exfoliation method has been vigorously employed due to several benefits such as simplest preparation set-up, less harmful chemicals use, low-cost technique, lower operating temperature and thickness control [1]. GO produced via electrochemical exfoliation method assisted by surfactant has paid an attention due to surfactant is able in changing or lowering the surface energy thus increase the interaction of the hydrophobic tail to the graphene materials to form stable colloidal system [2–4]. Commercially available surfactant sodium dodecyl sulphate (SDS) is commonly introduced in dispersing graphene-based materials in recent years [2,5]. Apart from surfactant role in determining the high quality of GO produced, the aids of applied voltage between the electrodes in the electrochemical system were highly needed where the method also relies on the electrical energy for the oxidation process. Based on the previous works, the applied voltage plays an important role on the GO production via electrochemical exfoliation method [1]. However, only a few researchers have been explored on the effect of applied voltage on the quality of GO produced via electrochemical exfoliation method [5].

Previous work found that the size of GO produced in the ionic liquid will decreased as the applied voltage increased [6]. This finding was related to the increasing number of GO layers by applying high voltage but low quality of GO. Meanwhile, Y Matsumoto et al. [7] shows the successfully production of GO at a very short time approximately < 1 h but suffers from extremely high applied voltage at 150 V. Hence, the excessive oxidation process might damage the honeycomb lattice structure of GO if the applied voltage was uncontrolled. Moreover, the honeycomb structure can also be affected by the insufficient oxidation process where a low production of GO was obtained. Due to the fact that the highest applied voltage gives the highest amount of GO produced, the appropriate applied voltage varied in the electrochemical exfoliation method was seen as one of the important parameter in order to control the quality and quantity for the GO production. The successfully controlled system by applying sufficient energy through applied voltage can paves the way for versatile approach in producing high quality and quantity of GO. This was due to the production of GO with low-cost and green synthesis method which involves low applied voltage is most favourable to be implemented in various applications. Due to the easily produced GO with an abundant amount in solution based, the used of GO as nanofillers in nanocomposites are considered as promising candidates to be used as electrode materials today due to the unique properties [8].

* Corresponding author at: Nano-Optoelectronics Research and Technology Laboratory, School of Physics, Universiti Sains Malaysia,11800 Minden Penang, Malaysia.
*E-mail address:* mdnurhafizah@usm.my (M.D. Nurhafizah).

https://doi.org/10.1016/j.diamond.2019.107624
Received 15 July 2019; Received in revised form 22 October 2019; Accepted 11 November 2019
Available online 12 November 2019
0925-9635/ 

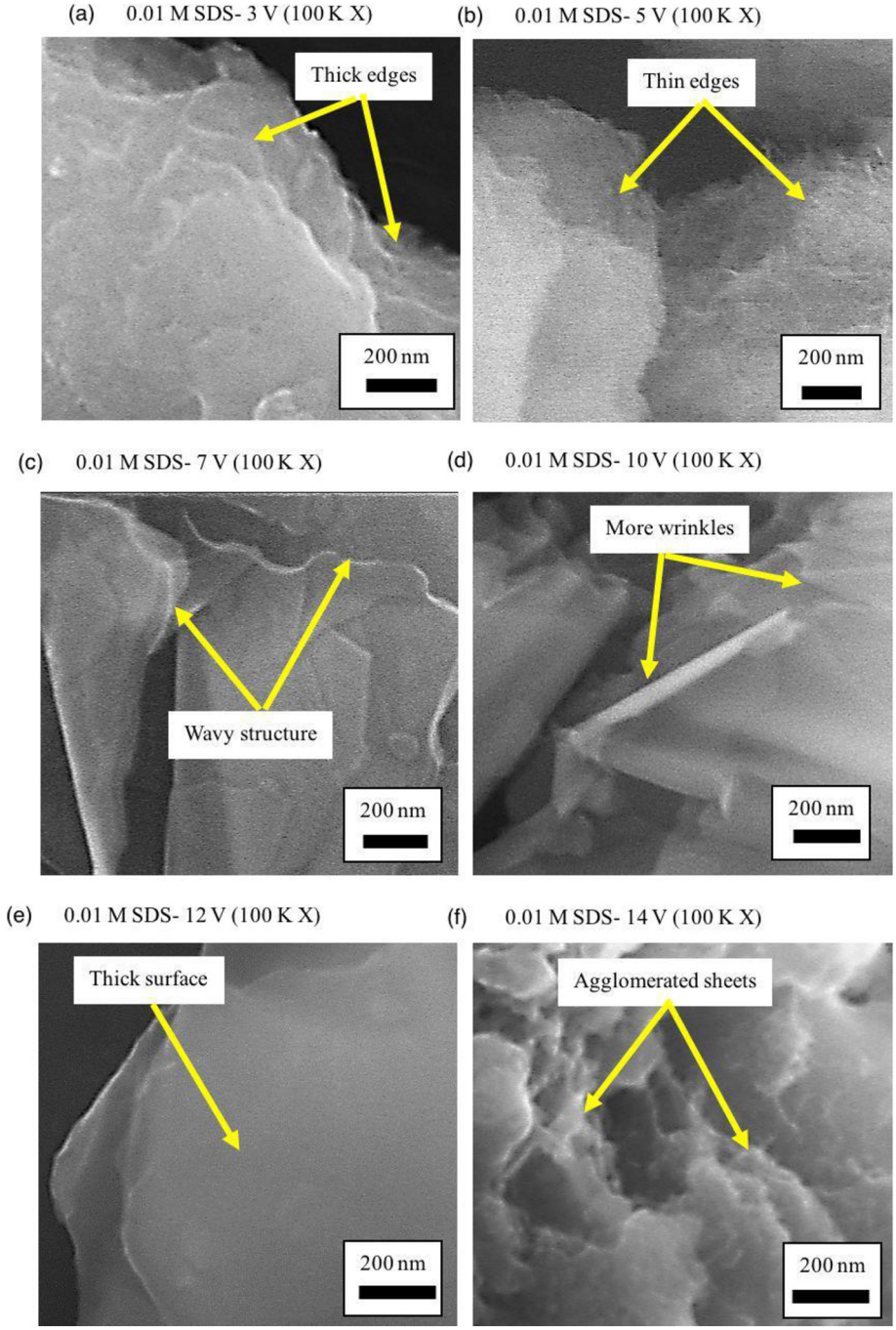


**Fig. 1.** FESEM images of GO synthesized at (a) 3, (b) 5, (c) 7, (d) 10, (e) 12, and (f) 14 V of applied voltage.

Currently, the selection of natural rubber latex (NRL) polymer as a host polymer is trending because the NRL polymer is one of the cheapest, readily available and water soluble polymer as compared to the synthetic rubbers. Since 1960s, the NRL polymer has shown outstanding properties particularly in mechanical strength and hardness [9]. Therefore, many attempts have been made in order to improve the NRL properties especially in electrical conductivity and further explore the possible potential of NRL-based nanocomposites. The systematic studies of the conductive electrodes from graphene-based NRL nanocomposites are important to overcome the limited used of natural sources for forthcoming applications. By taking the advantages of GO and NRL polymer, researches have introduced both materials to take the synergy effect of the materials for better nanocomposites production. However, the low conductivity and dispersibility of the nanocomposites, the introduction of surfactant is necessary for improving the interfacial adhesion in the nanocomposites. As previously reported, the introduction of surfactant gives an extra conductive pathway to the GO/NRL nanocomposites in order to simultaneously convert the insulating NRL polymer to the conductive nanocomposites [2].

To the best of our knowledge, there is no work reported on the effect of applied voltage on the GO production assisted SDS composited in the NRL polymer as conductive electrodes for supercapacitor application. In addition, a new fabrication method of GO/NRL nanocomposites also give benefits to the conductive electrodes production as this method demonstrate convenient, simple and innovative approach. Therefore, it was crucial to properly study on the important role of applied voltage on the production of GO through an electrochemical exfoliation method

and its application for supercapacitor electrodes. The greener, economical, flexible and conductive nanocomposites was highly demanded to be implemented as supercapacitor application.

## 2. Materials and methods

Prior to the fabrication of GO/NRL polymer nanocomposites via one-step method of electrochemical exfoliation as previously reported [10], the GOs were initially synthesized to investigate the optimum applied voltage on the production of high quality and quantity of the GO solution. The experimental set-up was followed from the previous work [6]. Two graphite rods (diameter: 10 mm and length: 15 cm, Model MV10) were immersed in the electrolyte solution containing sodium dodecyl sulphate (SDS) surfactant. The synthesis time was carried out at fixed 24 h for every set of applied voltage in the range of 3, 5, 7, 10, 12 and 14 V, respectively. The dispersion obtained was washed with ethanol and directly centrifuged at 5000 rpm for 30 min and dried at 80 °C overnight in an oven. In order to investigate the electrical conductivities, specific capacitance, and mechanical performances of the GO filled nanocomposites, the synthesized GOs were further fabricated via one-step method. The one-step fabrication method of GO/NRL nanocomposites was done by intermixing the NRL polymer into the GO production during electrochemical exfoliation method at synthesis time of 24 h. The thin films of nanocomposites were obtained by drop casted and dried in the $5 \times 5\,cm^2$ container at 60 °C.

## 3. Characterizations

The structural properties of the GO samples were characterized using field emission scanning electron microscopy (FESEM-Hitachi SU 8020), atomic force microscopy (X100), and micro-Raman spectroscopy (Renishaw InVia Raman Microscope) at excitation source of 514 nm and UV–Vis absorption spectroscopy (Agilent 8453 Spectrophotometer). The chemical composition was confirmed by Fourier transform infrared spectroscopy (Nicolet Macna-IR 760) within the region of 500 to 4000 $cm^{-1}$ using an attenuated total reflection (ATR) accessory. Meanwhile, for nanocomposites samples, four-point probe measurement (Keitley 2636A) and Gamry potentiostat series-G750 were used in order to investigate the electrical conductivities and capacitance performance of the samples. The nanocomposites samples of $1 \times 1\,cm^2$ were initially assembled with 1 M KOH electrolyte for capacitance measurement. Mechanical properties were obtained using a 50kN load cell universal tensile machine INSTRON5969 electronic tensile with computer control systems. The speed rate was 50 mm $min^{-1}$ at room temperature. Thermogravimetric analysis (Stare, Mettler Toledo and Perkin Elmer) was used to investigate the thermal stability of samples in nitrogen atmosphere.

## 4. Result and discussion

Fig. 1 shows the FESEM images of pristine GO samples produced at different synthesis voltages of 3, 5, 7, 10, 12, and 14 V, respectively. Below 5 V, a thick and non-exfoliated GO sheets was observed. This observation shows that the production of GO with thin and transparent sheets cannot be started at or below than 3 V of synthesis voltage due to insufficient energy to exfoliate the bulk graphite. For the GO sample produced at 5 V applied voltage, showed the slightly thin sheets. This might due to the medium rate of oxidation process caused to reduce the thick edges of GO sample to a slightly thin edges structure.

Meanwhile, once the higher voltage was applied in the range of 7 to 12 V, the structures of GO synthesized showed the crinkled silk-like sheets. The GO structures have a wavy characteristics resulted from the sufficient energy provided during oxidation process. This can be explained due to the high applied voltage of 7 V increases the rate of oxidation process and the GO sheets started to exfoliate into individual layers. However, the individual GO sheets observed were stacked layer by layer due to the intrinsic stacked structure and strong van der Waals interaction [11].

As compared to the GO sample synthesized at 7 V, the synthesized GO at 10 V showed more wrinkles structures indicating high successfully exfoliation process. The sheets were thinner than the former GO produced at 7 V. This confirmed that the GO was more oxidized at a higher applied voltage. This can be seen from the folded upward of the GO edges. In the case of GO sample synthesized at 12 V, the GO structures were observed to have a thick surface but the folded structures can still be observed from the sample resulting due to oxidation process.

This observation shows that by increasing the applied voltage to 12 V, the high amount of GO was produced therefore the GO layers were started to stack on the middle surface due to strong van der Waals interaction between the GO sheets [9,12]. The abundance of oxygen functional groups anchored above and below the GO structures has caused bright GO structures [13]. This showed that the oxidation process through the exfoliation techniques was rapidly occurred.

However, at higher applied voltage of 14 V, a very thick agglomeration of GO sheets was detected as pointed by arrows. The GO sample was seen to have crack-like structures on the GO structures which was believed due to the elastic strain energy build-up in the sheets during oxidation [14]. The increasing amount of GO produced were convinced by the transition colour from light yellow to dark solution as the applied voltage was increased from 3 to 14 V (see Supplementary). Generally, the absorption spectra show the appearance peaks at around 224–232 nm. The existence peaks confirmed that the oxygen functional groups have increased the graphite layer that was correlates to the π-π* transition of C═C in GO. The morphology results were supported by AFM images.

For AFM measurement (Fig. 2), the GO samples were drop-casted onto freshly cleaved mica substrates. Generally, the distortions shown by AFM images are due to the relative sharpness of the tip and the surface features of the sample [15]. The thickness of the GO sample was in the range of 1–107 nm. This indicates that the formation of multilayers of graphene sheets increases due to the increasing oxidation level introduced during the exfoliation process. Note that the gap between surfactant and graphene sheets is ~0.3 nm [16]. The graphene film was not uniform, as its thickness varied considerably at different locations. Obviously, a uniform distribution with low-agglomerated GO samples was observed at above 5 to 10 V. In this case, the average thickness of layers GO was not an optimum measurement due to their various sizes, with non-parallel GO sheets stacked on each other onto the substrate.

However, the average thickness of the GO sheets was considerably higher than that of the GO produced in previous work [17] contrary to the GO sample produced at 3 V (~1 nm). The lowest average thickness might be due to the difficulty of the cantilever to detect the agglomerated structures consequence from the lowest amount of GO produced. Meanwhile, the highest roughness was observed to be due to the insertion of various amount of oxygen functional groups and the insertion of SDS surfactant in between the graphene layers. The summarized roughness data and applied voltage are presented in Fig. 2(g). The higher thickness was shown by the GO sample produced using 14 V due to the highly restacking of GO sheets with the higher amount of GO sheets produced. These results support the FESEM images shown on the various structures and the increasing amount of stacking GO layers as applied voltage is increased.

Fig. 3(a) shows the micro-Raman spectra of the GO obtained. Micro-Raman spectroscopy was employed for the GO samples due to the powerful non-destructive tool to characterize the ordered and disordered crystal structures. The two main peaks of carbon materials, D-peaks (~1350.9–1361.6 $cm^{-1}$) and G-peaks (~1586.8–1598.2 $cm^{-1}$) were detected in all samples. The G- and D-peaks were arising from the first order scattering of the $E_{2g}$ phonon of $sp^2$-bonded carbon atoms and the latter originates from the defects [4,5]. Therefore, the difference in

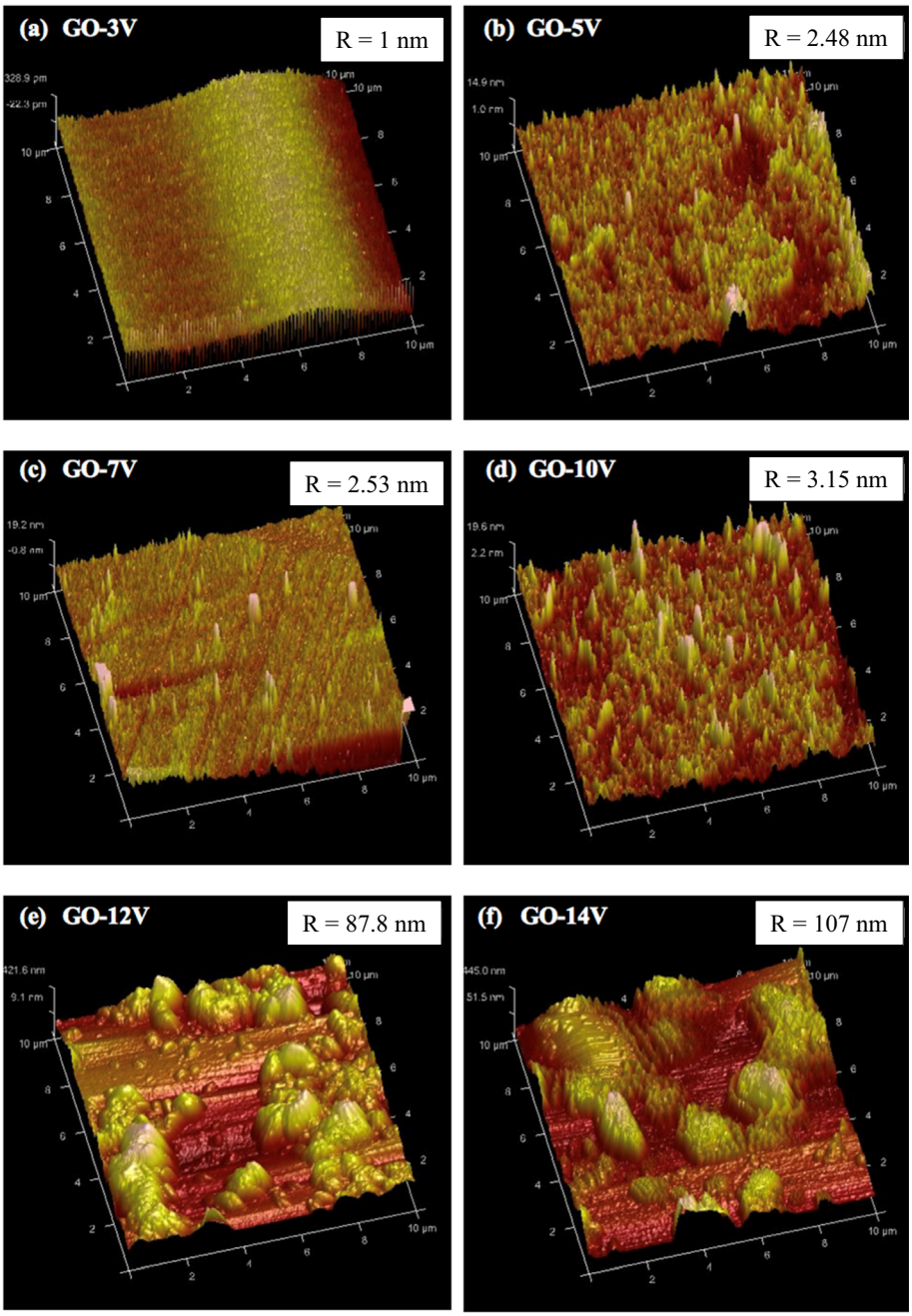


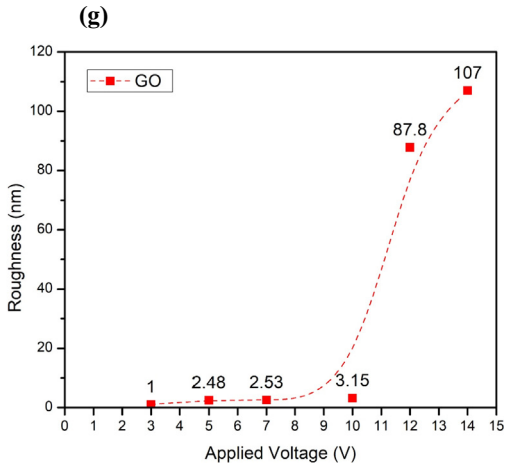


**Fig. 2.** AFM images of GO synthesized at different applied voltages of 3, 5, 7, 10, 12, and 14 V.

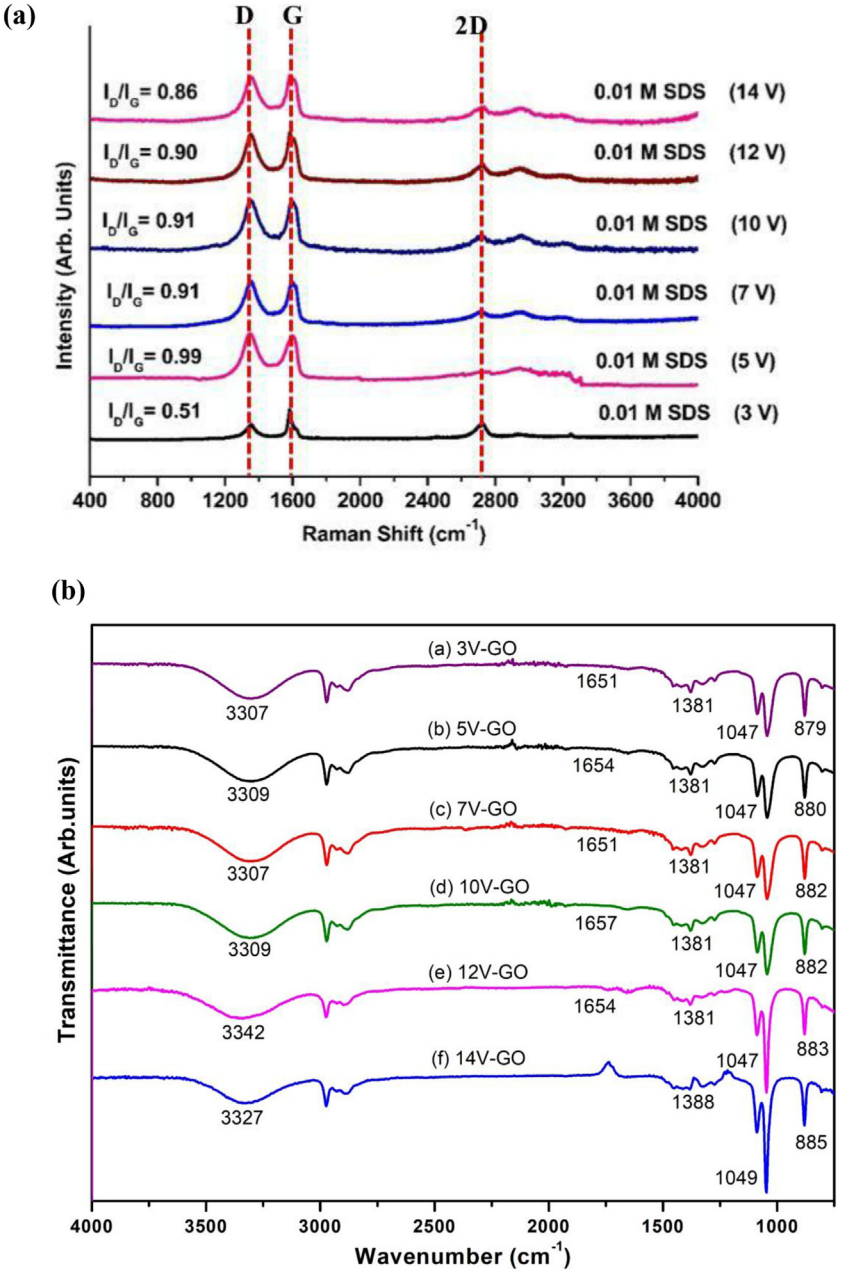


**Fig. 3.** (a) Micro-Raman of GO synthesized at different applied voltages of 3, 5, 7, 10, 12, and 14 V.
(b) FTIR spectra of GO synthesized at different applied voltages of 3, 5, 7, 10, 12, and 14 V.

their intensity ratio was important to be measured. The GO sample prepared at 3 V shows lowest $I_D/I_G$ ratio of 0.51. The existence of sharp G-peak at 1586.8 $cm^{-1}$ indicated that the GO sample produced was graphite-like structure due to insufficient energy. By increasing the applied voltage from 3 to 5 V, the value of $I_D/I_G$ ratio were increased. This was due to the size of GO surface decreasing as the edge defects increased, leading to the detection of higher defect intensity [18]. This was shown by the highly wrinkled of GO structure (5 V applied voltage), which contributed to the disordered structure which caused the increase in the $I_D/I_G$ ratio. However, when the applied voltage was further increased from 5 to 12 V, the $I_D/I_G$ ratio subsequently decreased from 0.99 to 0.90. This was attributed to the high number of openings in the layer of graphite via the high force of electric field provided from 5 to 12 V. This was proven by the FESEM images (Fig. 1).

The high voltage applied for the graphite rod in weakening the GO layers has led a number of exfoliated GOs produce. Moreover, the low number of wrinkles with folded structures observed in the GO samples indicate that the decrease in the edge defects also contributed to the decrease in the intensity of D- to G-peaks. In addition, the low calculated of $I_D/I_G$ ratio below 1 in every GO samples indicated that the samples have low defects and residual oxygen functional groups after the oxidation process, making it acceptable for further implement in aqueous and non-aqueous applications [19]. This observation supported the FESEM where a well-separated GO was produced (at 7–10 V) but an agglomerated GO structure was started to observe at ≥12 V. However, the edge defects give an advantage to the electrochemical systems and perhaps can increase the conductivities and the capacitance of the nanocomposites produced.

Further chemical characterization of the GO samples produced was carried out by FT-IR spectroscopy. Further increases in oxidation level by increasing the applied voltage from 3 to 14 V, the FT-IR spectra in Fig. 3(b) shows the presence of the oxygen-containing functional groups

that were successfully attached to the GO surfaces. A previous study has reported that the GO sheets is highly attached by the epoxy, hydroxyl, carbonyl and carboxyl groups [20]. Several prominent peaks were detected in the overall GO samples at 1047–1049 $cm^{-1}$ and 1381–1388 $cm^{-1}$, which represent the existence of epoxy and hydroxyl groups, respectively [21]. However, the intensity of the epoxy peaks can be clearly observed for the GO samples prepared using higher voltages at 12 and 14 V. This implies that the oxygen functional groups increased as the applied voltage increased. In addition, a broad and intense peak was observed at 3307–3342 $cm^{-1}$ (hydroxyl, OH) indicated the absorption of water molecules while the peak centred at around ~2970–2975 $cm^{-1}$ is attributed to C—H stretching in the GO sample produced using 3, 5, 7, 10, 12, and 14 V [22].

As the applied voltage increased, the O—H peak was observed to slightly shift from 3307 $cm^{-1}$ to 3342 $cm^{-1}$, indicating that the GO sample prepared at higher applied voltage expanded the graphite interlayer more than the prepared GO using lower applied voltage. The expanded graphite made the absorption of water molecules easier, and the SDS surfactant was subsequently inserted during the intercalation process [5]. However, the shifted peak from 3342 $cm^{-1}$ to 3327 $cm^{-1}$ for the 14 V-GO sample indicates that a higher amount of GO was produced; thus, the GO sample tends to re-agglomerate and become distorted. The presence of small carbonyl and carboxyl peaks at 1651–1657 $cm^{-1}$ further confirmed that the various applied voltages affected the degree of oxidation level for each GO sample [23]. However, the inconsistent peak evolved in all GO samples, except for 14 V-GO sample, due to the variation of the edges GO structures as convinced by FESEM image. Meanwhile, the peaks of the carbonyl groups in the lower range was slightly shifted from 879 $cm^{-1}$ to 885 $cm^{-1}$ due to the increased oxidation and intercalation processes during the electrochemical exfoliation method [24].

## 5. *I-V* conductivity

The electrical conductivity of the GO/NRL nanocomposites were explained by the current-voltage characteristic graph in Fig. 4. The incremental pattern of the electrical conductivities for all nanocomposites were observed, contrary to the 3 V-GO/NRL nanocomposites (inset figure), for which the lowest conductivity ($4.43 \times 10^{-12}$ S $cm^{-1}$) was calculated due to the low quantity of 3 V-GO consumed. This made the nanocomposites become very close to the electrical conductivity of pure NRL [25]. By increasing the applied voltage from 3 to 5 V for GO production, dramatic increases in the electrical conductivity were observed ($\sigma = 1.66 \times 10^{-5}$ S $cm^{-1}$). This was due to the synthesized GO sheets starting to build a conductive pathway within the nanocomposite sample.

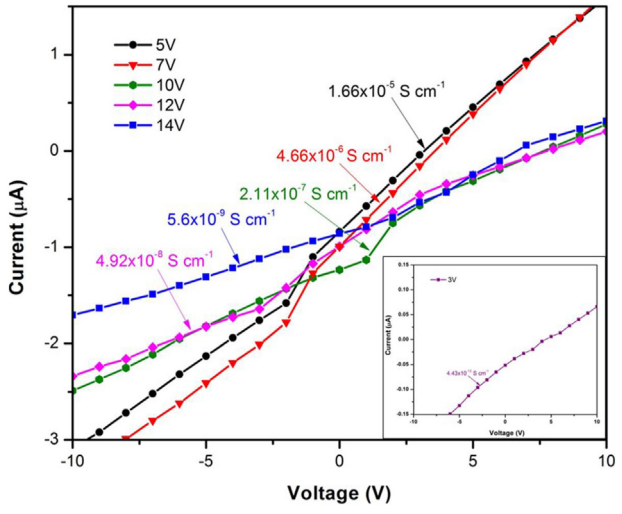


**Fig. 4.** *I-V* curves of SDS-GO/NRL polymer nanocomposite synthesized at 3, 5, 7, 10, 12, and 14 V.

The electrical improvement is believed to be due to the following factors: (1) an appropriate amount of GO produced under various applied voltages which reflected from the successful degree of oxidation process; (2) the amount of effective interfacial interactions between the SDS-GO sheets and NRL matrix; and (3) the high level of dispersion GO in the nanocomposite makes the nanocomposite produced become electrically conductive. However, the decrement pattern of the electrical conductivity was observed as the applied voltage is increased (5 to 14 V). The result demonstrated that the greater amount of GO produced during the exfoliation process influenced the lower conductivity of nanocomposites obtained. For example, the GO/NRL nanocomposite synthesized at above 12 V shows a slightly lower electrical conductivity of $\sim \times 10^{-8}$ to $\times 10^{-9}$ S $cm^{-1}$ as compared to the 7 V- and 10 V-GO/NRL nanocomposites ($\sim \times 10^{-6}$ to $\times 10^{-7}$ S $cm^{-1}$). It is worth noting that, the dramatically decreased of electrical conductivity was attributed to the higher and rapid oxidation degree from 5 to 14 V [26]. The higher amount of oxygen functional groups might affect the electron movement in the GO and caused difficult formation of conductive pathway in nanocomposite. The electrons confined in the agglomerated GO structures were believed to rarely tunnel from the inner to the outer part of GO in the nanocomposite to form efficient conductive network between the GO neighbours. These results were supported by FESEM, AFM, and micro-Raman analysis for GO production.

## 6. *C-V* measurement

Fig. 5 shows the GO/NRL nanocomposites samples synthesized at various applied voltages from 3 to 14 V. From the results, all prepared GO/NRL nanocomposites show a leaf-like shape correspond to the good ability restoring charges. However, among these, 5 V-GO/NRL nanocomposites exhibited the highest current response (~7 mA) with calculated specific capacitances up to 103 F $g^{-1}$. The wrinkles GO showed in FESEM image created higher reactive site for interaction of hydrogen bond between the oxygen functional groups in GO and the hydroxyl group in NRL polymer. Moreover, the van der Waals interaction between the SDS and the GO surface in addition to the hydrogen-bonding between the GO sheets and the NRL polymer also increased the pathway for the ions transferred.

This resulted in increased ions movement and charge storage in the supercapacitor as shown by cyclic measurement. This meant that the electrochemical performances of the GO/NRL nanocomposite were enhanced due to the higher amount of effective synergy between the GO dispersions and the NRL polymer matrix [27,28]. This result was consistent with the higher electrical conductivity obtained. However, per Fig. 5(d) (10V-GO/NRL nanocomposite), a slightly non-linear C-V graph was detected, which might be due to the excessive GO sheets accumulating and blocking the active surfaces of nanocomposites for ion diffusion then led to capacity loss and lower electrical conductivity ($\times 10^{-7}$ S $cm^{-1}$) obtained. The decrement pattern of specific capacitance was continuously observed as the applied voltage increased. This further confirmed the existence of bulk GO sheets agglomerated in the nanocomposites making the ions trapped within the structures proportionally reduce the performance.

## 7. Mechanical measurement

The dumbbell nanocomposites samples as shown in inset Fig. 6 were further investigated. The mechanical properties of the nanocomposites, such as tensile strength and modulus, were investigated, and depicts in stress-strain curve as shown in Fig. 6. As GO loading increased, both the tensile strength ($\sigma_b$) and Young Modulus (E) increased, but the elongation at break (EB) of the nanocomposites decreased. From the results, when the applied voltage increased, the $\sigma_b$ and E increased from 0.1973–0.4176 MPa and 2490–20,200 MPa, respectively. The results

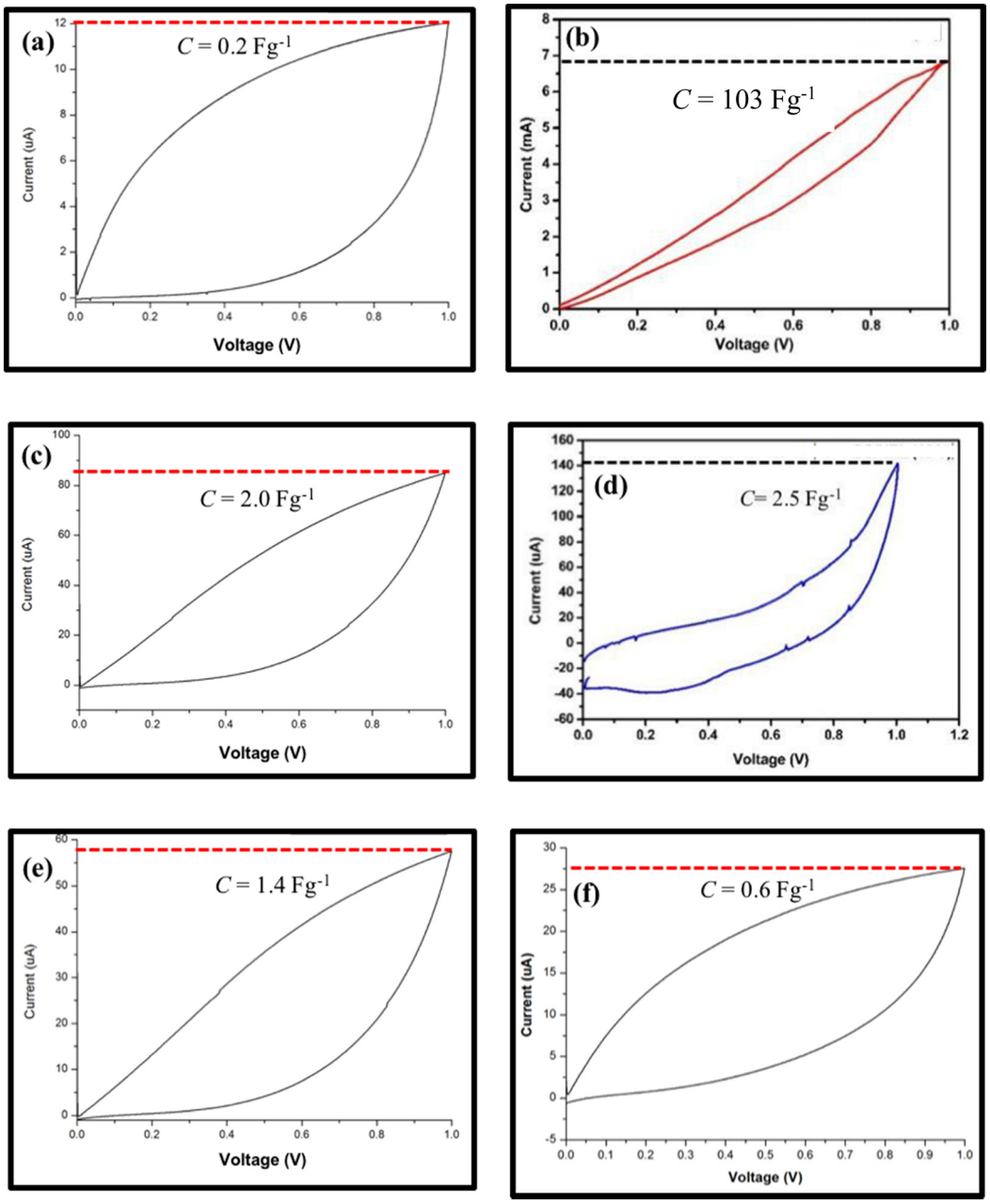


**Fig. 5.** *C-V* curves of SDS-GO/NRL polymer nanocomposite synthesized at 3, 5, 7, 10, 12, and 14 V.

suggested that the GO produced could improve the strength and stiffness of NRL nanocomposites at the expense of flexibility, similar to previous reports [29,30]. For example, the improvement in the mechanical properties was observed at below 7 V of applied voltage for the fabrication GO/NRL nanocomposites due to the good dispersion of low-agglomerated GO within the NRL matrix and the strong interfacial interactions between the GO and NRL matrices, as convinced by FESEM images. When the nanocomposites were under tensile stress, the fillers were difficult to disconnect from the matrix, and could resist and transfer the imposed force, leading to the weakening of the loading stresses of NRL matrix [31]. However, the $\sigma_b$ of the GO/NRL nanocomposites are slightly lower than previous reported work, which may be attributed to the fact that it is difficult to separate the agglomeration GO during mechanical mixing, especially for the higher applied voltages (above 10 V) [32]. In addition, the slightly difference pattern observed for the 3 V-GO/NRL nanocomposite, which might be attributed to the amount of GO consumed in the nanocomposite, is below the percolation point [33], resulting in a lower $\sigma_b$ value. In other case, the higher interaction between GO in NRL matrix led to the higher force needed to stretch the nanocomposites to a certain elongation, so adding GO significantly decreased EB of the nanocomposites. These results are complimentary to the electrical conductivities and capacitance performance of the nanocomposites, as, the appropriate amount of GO sheets will strongly affect the overall performances of the nanocomposites. A summary of electrical, specific capacitance, and mechanical testing is tabulated in Table 1.

## 8. Nanocomposite morphology

Fig. 7 shows the FESEM micrographs of GO/NRL polymer nanocomposite synthesized at 5 and 10 V. The GO sheets synthesized at 5 V were highly exfoliated in the NRL polymer matrix through the one-step method. There were many outcrops of the broken GO on the surface of the nanocomposite. The results observed were due to the strong

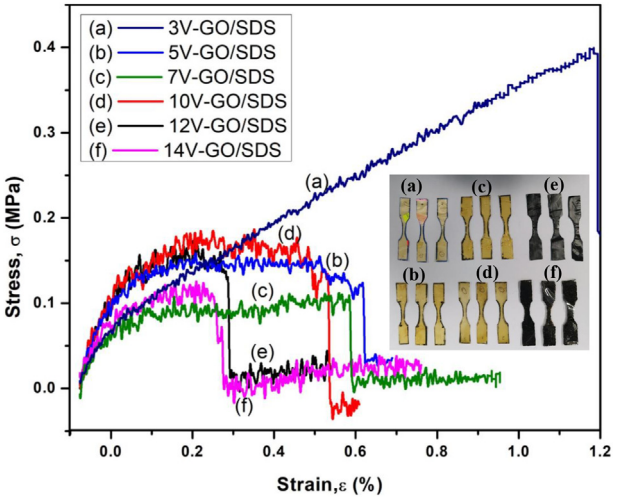


**Fig. 6.** Mechanical testing of polymer nanocomposite synthesized at 3, 5, 7, 10, 12, and 14 V.

interaction between the GO and NRL polymer matrix which might be attributed to the various functional groups located on the surface of GO [34].

The highly wrinkled GO shown in the FESEM image offers a higher possibility of increased of hydrogen-bonding interaction between the oxygen groups in GO structures and the hydroxyl group in NRL polymer. Moreover, the attachment of SDS surfactant to the GO structures also might increase the van der Waals interaction of SDS-GO, leading to the higher interaction and higher electrical conductivity.

Meanwhile, the SDS-GO/NRL polymer nanocomposite synthesized at 10 V shows a rougher surface and larger agglomerated GO sheets on the nanocomposite surface. In addition, the presence of agglomerated GO sheets forced crack formation, as detected in several parts as shown by small arrows. Therefore, when the agglomeration GO was obviously seen, the conductive pathways between the GO sheets and NRL matrix is seen to be less effective due to the limited reactive sites for hydrogen-bonding formation, thus leading to slightly lower electrical conductivity. Due to this, the proper selection of applied voltage with sufficient amount of SDS surfactant to fabricate GO/NRL polymer nanocomposite also had a significant effect on the electrical, capacitance and structural properties of the nanocomposite produced.

Fig. 8 shows the micro-Raman spectra of the 0.01 M SDS-GO/NRL polymer nanocomposite samples. All prepared samples showed a red-shifted peak of D- and G-peaks in the range of 1352.9–1368.4 and 1523.0–1579.1 $cm^{-1}$, respectively. Generally, the addition of GO dispersions in the NRL polymer matrix caused the $I_D/I_G$ ratios to increment in the nanocomposites produced.

To further understand the effects of different applied voltage on the GO production and its nanocomposites, TGA was used to evaluate the thermal stability and decomposition of the residual functional groups in the prepared samples. Fig. 9(a) depicts the TGA for GO production at 7, 10, 12 and 14 V, with three-step major weight losses was found at around 150, 250 and 450 °C, except for 3 and 5 V-GO, where only two major steps weight losses at ~150 and ~300 °C are observed. The thermal decomposition of species is dictated by the bond dissociation energies which follows the order, weakly bound water due to H-bonding < C—O—C (epoxides), COOH, OH—C—C—OH < ketones, C—C < C═C [13]. An onset decomposition at below 150 °C can be attributed to the removal of water molecules [21]. This was shown by all GO samples.

Then, the second weight loss between the 150–300 °C was due to the decomposition of —OH and ═O [35]. The GO sample produced using 3 and 5 V showed a major decomposition at this region with calculated weight loss at ~84.24 and ~85.310 wt%, respectively, which might be due to the low amount of GO produced consequent from the moderate exfoliation and intercalation processes occurred at this applied voltage. This subsequently confirmed the low amount of oxygen functional groups existed in the GO structures as convinced by the edges sheets showed by FESEM images. Meanwhile, the third major weight loss at around 300–450 °C was attributed to the dissociation of remaining unstable carbon structure [35]. By increasing the applied voltage, the centred band of the decomposition is shifted to a slightly higher at ~450 °C, corresponding to the increased production of GO sheets; thus, more types of oxygenises functional groups are attached to the GO sample. The GO samples synthesized at 3 and 5 V were observed to burn up at above 350 °C with residual weight loss of ~3-8 wt% as compared to GO synthesized using 7–14 V, were burnt up at around 400 °C (~10–20 wt%). The residual weight loss at this region was due to the nature behaviour of GO affected by the synthesis process [36]. The result was in a good agreement with FESEM, AFM, micro-Raman, and FT-IR analysed. From the results, the optimum GO samples with good quality and quantity were shown by 5 and 10 V of applied voltage.

Therefore, in Fig. 9(b), the comparison was made between the pristine GO, pure NRL, and GO/NRL nanocomposite synthesized at 5 and 10 V. In general, it was revealed that both GO/NRL polymer nanocomposite samples remain stable at least until 350 °C. The slight decrease in the thermal stability of the GO/NRL polymer nanocomposite synthesized at 5 V as compared to the pristine GO and pure NRL polymer indicates that the highly wrinkled GO efficiently diffused in the nanocomposite, increasing the interaction with the NRL polymer. This also contributed to the enhancement of electrical conductivity ($\sim \times 10^{-5}$ S $cm^{-1}$) and capacitance performance ($C = 103$ F $g^{-1}$). In comparison, the agglomerated GO structures produced using higher applied voltage of 10 V during electrochemical exfoliation method lead to the partially diffused GO sheets in the nanocomposite and low interaction between the GO and the NRL polymer, thus slightly affecting thermal stability to make the nanocomposite more stable. Even though the higher applied voltages (10 V) in nanocomposite production used lead to greater thermal stability than the nanocomposite produced at 5 V, the GO/NRL polymer nanocomposite produced at 5 V shows better interaction between the GO sheets and the NRL polymer due to the low agglomeration GO sheets.

The proposed mechanism of the electrical conductivity

**Table 1**
Summarized of GO/NRL nanocomposite produced using different applied voltage.

| Sample description | Electrical conductivity, $\sigma$ ($Scm^{-1}$) | Specific capacitance, Cs ($Fg^{-1}$) | Mechanical test | | | |
|---|---|---|---|---|---|---|
| | | | Max load (N) | Tensile strength, $\sigma_b$ (MPa) | Young modulus, E (MPa) | Elongation at break, EB (%) |
| 3 V-GO/NRL | $4.43 \times 10^{-12}$ | 0.2 | 0.51124 | 0.1973 | 2490 | 115 |
| 5 V-GO/NRL | $1.66 \times 10^{-5}$ | 103 | 0.52632 | 0.2009 | 3110 | 89.4 |
| 7 V-GO/NRL | $4.66 \times 10^{-6}$ | 2.0 | 0.74663 | 0.2083 | 5360 | 72.8 |
| 10 V-GO/NRL | $2.11 \times 10^{-7}$ | 2.5 | 0.48072 | 0.2380 | 8950 | 66.6 |
| 12 V-GO/NRL | $5.60 \times 10^{-8}$ | 1.4 | 0.63853 | 0.2460 | 13,200 | 59.5 |
| 14 V-GO/NRL | $4.92 \times 10^{-9}$ | 0.6 | 1.93 | 0.4176 | 20,200 | 53.6 |

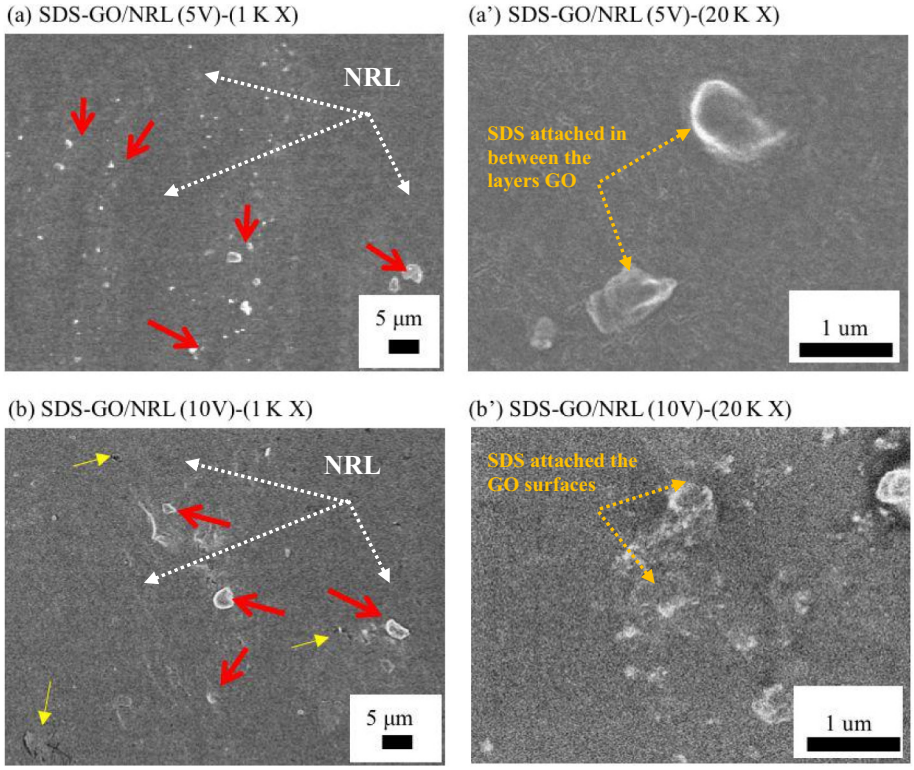


**Fig. 7.** FESEM images of SDS-GO/NRL (5 and 10 V) polymer nanocomposite.

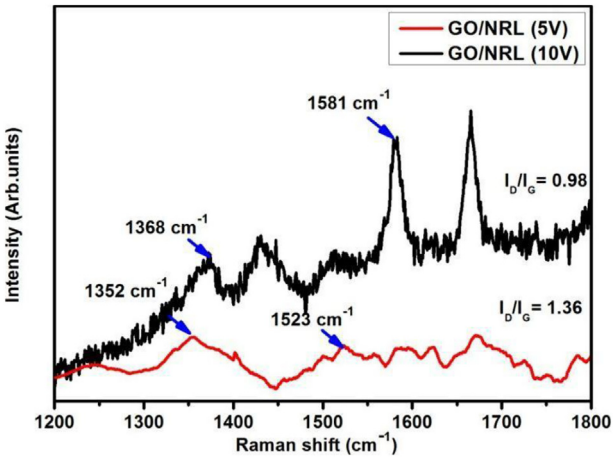


**Fig. 8.** Micro-Raman spectra of SDS-GO/NRL (5 and 10 V) polymer nanocomposites.

enhancement of the nanocomposite is basically followed from the previous work [37]. A typical synthesized GO usually loaded with an abundance of oxygen functional groups such as carbonyl, carboxyl, epoxy, and hydroxyl at the basal plane and the edges structure [38]. The oxygenises groups containing on the GO surface sometimes has hindered the low surface tension of SDS to have free access onto all regions GO which led to a minimum attachment of SDS tail to the GO structure. This contributes to the only slightly improved electrical conductivity for both nanocomposites. However, the nanocomposite synthesized at 5 V shows higher electrical conductivity ($\times 10^{-5}$ S cm$^{-1}$) which was believed due to the formation of more conductive web connections because of the low amount GO produced containing minimum functional groups on the surfaces during the oxidation process. This also led to the higher capacitive value due to the layered-structure of GO produced allows the kinetic movement of ion between the electrodes.

## 9. Conclusion

In summary, GO/NRL polymer nanocomposite was successfully synthesized under various applied voltage from 3 to 14 V via one-step method of electrochemical exfoliation. For pristine GO, a highly wrinkles structures and moderate crystallinity ($I_D/I_G$ = 0.91) was successfully synthesized at 10 V of applied voltage. On the other hand, the synthesis of GO/NRL polymer nanocomposite at 10 V showed better dispersions obtained with moderate crystallinity ($I_D/I_G$ = 0.98). Meanwhile, the effect on the dispersion can be further measured in the electrical conductivities increment for the GO/NRL nanocomposites synthesized in the ranges of 5 to 10 V ($\sigma = \sim \times 10^{-7}$ to $\sim \times 10^{-5}$ S cm$^{-1}$). In addition, the overall nanocomposite sample showed potential in the supercapacitor performance through the *C-V* and mechanical analyses. The use of one-step method in the fabrication of GO/NRL polymer nanocomposite was believed to be easier, cost-effective and greener because this process efficiently intermixed the exfoliated GO and NRL polymer in one time during the exfoliation process via electrochemical exfoliation method.

## Declaration of competing interest

The authors declare no competing financial interest.

## Acknowledgements

This work is funded by Short Term Grant (Grant code: 304/PFIZIK/6315241), and Tabung Persidangan Luar Negara (Grant code: 302/JPNP/312001), Universiti Sains Malaysia (USM). Authors want to thank Nano-Optoelectronics Research and Technology Laboratory (USM), Science and Engineering Research Centre (SERC-USM), and Universiti Pendidikan Sultan Idris (UPSI) for the facilities support. Many thanks to Dr. Azira Abd Aziz from Malaysia Rubber Board for

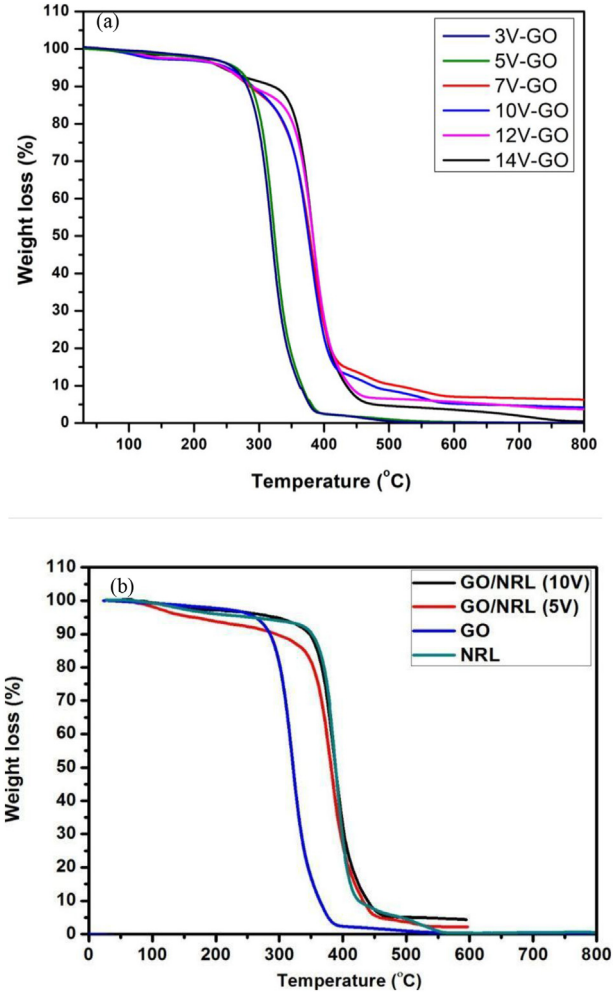


**Fig. 9.** TGA curves of (a) GO synthesized at 3, 5, 7, 10, 12, and 14 V and (b) SDS-GO/NRL (5 and 10 V) polymer nanocomposite.

supplying the natural rubber latex polymer to support the work.

## Appendix A. Supplementary data

Supplementary data to this article can be found online at https://doi.org/10.1016/j.diamond.2019.107624.

## References

[1] G. Wang, B. Wang, J. Park, Y. Wang, B. Sun, J. Yao, Highly efficient and large-scale synthesis of graphene by electrolytic exfoliation, Carbon 47 (14) (2009) 3242–3246.
[2] A. Mohamed, T. Ardyani, A.B. Suriani, P. Brown, M. Hollamby, M. Sagisaka, J. Eastoe, Graphene-philic surfactants for nanocomposites in latex technology, Adv. Colloid Interf. Sci. 230 (2016) 54–69.
[3] K. Kakaei, K. Hasanpour, Synthesis of graphene oxide nanosheets by electrochemical exfoliation of graphite in cetyltrimethylammonium bromide and its application for oxygen reduction, J. Mater. Chem. A 2 (37) (2014) 15428–15436.
[4] M. Alanyahoğlu, J.J. Segura, J.O. Solé, N.C. Pastor, The synthesis of graphene sheets with controlled thickness and order using surfactant-assisted electrochemical processes, Carbon 50 (2012) 142–153.
[5] M.D. Nurhafizah, A.B. Suriani, S. Alfarisa, A. Mohamed, I.M. Isa, A. Kamari, N. Hashim, A.A. Aziz, M.R. Mahmood, The synthesis of graphene oxide via electrochemical exfoliation method, Adv. Mater. Res. Trans Tech Publ. 1109 (2015) 55–59.
[6] J. Lu, J.-x. Yang, J. Wang, A. Lim, S. Wang, K.P. Loh, One-pot synthesis of fluorescent carbon nanoribbons, nanoparticles, and graphene by the exfoliation of graphite in ionic liquids, ACS Nano 3 (8) (2019) 2367–2375.
[7] Y. Matsumoto, H. Tateishi, M. Koinuma, Y. Kamei, C. Ogata, K. Gezuhara, K. Hatakeyama, S. Hayami, T. Taniguchi, A. Funatsu, Electrolytic graphene oxide and its electrochemical properties, J. Electroanal. Chem. 704 (2013) 233–241.
[8] G.Z. Papageorgiou, Z. Terzopoulou, D. Bikiaris, K.S. Triantafyllidis, E. Diamanti, D. Gournis, P. Klonos, E. Giannoulidis, P. Pissis, Evaluation of the formed interface in biodegradable poly (L-lactic acid)/graphene oxide nanocomposites and the effect of nanofillers on mechanical and thermal properties, Thermochim. Acta 597 (2014) 48–57.
[9] L. Yue, G. Pircheraghi, S.A. Monemian, I.M. Zloczower, Epoxy composites with carbon nanotubes and graphene nanoplatelets-dispersion and synergy effects, Carbon 78 (2014) 268–278.
[10] A.B. Suriani, M.D. Nurhafizah, A. Mohamed, A.K. Masrom, V. Sahajwalla, R.K. Joshi, Highly conductive electrodes of graphene oxide/natural rubber latex-based electrodes by using a hyper-branched surfactant, Mater. Des. 99 (2016) 174–181.
[11] J.K.W. Sandler, J.E. Kirk, I.A. Kinloch, M.S.P. Shaffer, A.H. Windle, Ultra-low electrical percolation threshold in carbon-nanotube-epoxy composites, Polym. J. 44 (19) (2003) 5893–5899.
[12] F. Tavakoli, M. Salavati-Niasari, F. Mohandes, Green synthesis and characterization of graphene nanosheets, Mater. Res. Bull. 63 (2015) 51–57.
[13] S. Pan, I.A. Aksay, Factors controlling the size of graphene oxide sheets produced via the graphite oxide route, ACS Nano 5 (5) (2011) 4073–4083.
[14] J. Yan, J. Liu, Z. Fan, T. Wei, L. Zhang, High-performance supercapacitor electrodes based on highly corrugated graphene sheets, Carbon 50 (6) (2012) 2179–2188.
[15] J. Shen, B. Yan, M. Shi, H. Ma, N. Li, M. Ye, One step hydrothermal synthesis of TiO2-reduced graphene oxide, J. Mater. Chem. 21 (2011) 3415–3421.
[16] S. Sadhukan, T.K. Ghosh, I. Roy, D. Rana, A. Bhattacharyya, R. Saha, S. Chattopadhyay, S. Khatua, K. Acharya, D. Chattopadhyay, Green synthesis of cadmium oxide decorated reduced graphene oxide nanocomposites and its electrical and antibacterial properties, Mater. Sci. Eng. C. 9 (2019) 696–709.
[17] A. Hadi, J. Zahirifar, J. Karimi-Sabet, A. Dastbaz, Graphene nanosheets preparation using magnetic nanoparticle assisted liquid phase exfoliation of graphite the coupled effect of ultrasound and wedging nanoparticles, Ultrason. Sonochem. 44 (2018) 204–214.
[18] J. Xu, Z. Shi, X. Zhang, G.M. Haarberg, Mechanism of graphene formation by graphite electro-exfoliation in ionic liquids-water mixtures, Mater. Res. Express. 1 (4) (2014) 045606.
[19] N.-W. Pu, C.-A. Wang, Y.-M. Liu, Y. Sung, D.-S. Wang, M.-D. Ger, Dispersion of graphene in aqueous solutions with different types of surfactants and the production of graphene films by spray or drop coating, J. Taiwan Inst. Chem. Eng. 43 (1) (2012) 140–146.
[20] M.V. Narayana, S.N. Jammalamadaka, Tuning optical properties of graphene oxide under compressive strain using wet ball milling method, Graphene 5 (02) (2016) 73–80.
[21] N. Yadav, B. Lochab, A comparative study of graphene oxide: hummers, intermediate and improved method, Flatchem 13 (2019) 40–49.
[22] W. Fan, C. Zhang, W.W. Tjiu, T. Liu, Fabrication of electrically conductive graphene/polystyrene composites via a combination of latex and layer-by-layer assembly approaches, J. Mater. Res. 28 (04) (2013) 611–619.
[23] G. Venugopal, K. Krishnamoorthy, R. Mohan, S.J. Kim, An investigation of the electrical transport properties of graphene-oxide thin films, Mater. Chem. Phy. 132 (1) (2012) 29–33.
[24] H.L. Guo, X.F. Wang, Q.Y. Qian, F.B. Wang, X.H. Xia, A green approach to the synthesis of graphene nanosheets, ACS Nano 3 (9) (2009) 2653–2659.
[25] M. Ab Rahman, G.B. Tong, N.H. Kamaruddin, F.A. Wahab, N.A. Hamizi, Z.Z. Chowdhury, S. Sagadevan, N. Chanlek, M.R. Johan, Effect of graphene infusion on morphology and performance of natural rubber latex/graphene composites, J. Mater. Sci. Mater. El. 30 (2019) 12888–12894.
[26] Q.-L. Meng, H.-C. Liu, Z. Huang, S. Kong, X. Lu, P. Tomkins, P. Jiang, X. Bao, Mixed conduction properties of pristine bulk graphene oxide, Carbon 101 (2016) 338–344.
[27] H. Yu, B. Zhang, C. Bulin, R. Li, R. Xing, High-efficient synthesis of graphene oxide based on improved hummers method, Sci. Rep. 6 (2016) 36143.
[28] J. Lyu, M. Mayyas, O. Salim, H. Zhu, D. Chu, R.K. Joshi, Electrochemical performance of hydrothermally synthesized rGO based electrodes, Mater. Today Energy 13 (2019) 277–284.
[29] Y.G. Yu, J.W. Yang, B.X. Liu, X.F. Ma, Preparation and characterization of glycerol plasticized-pea starch/ZnO-carboxymethylcellulose sodium nanocomposites, Bioresour. Technol. 100 (2009) 2832–2841.
[30] Y. Zhan, M. Lavorgna, G. Buonocore, H. Xia, Enhancing electrical conductivity of rubber composites by constructing interconnected network of self-assembled graphene with latex mixing, J. Mater. Chem. 22 (21) (2012) 10464–10468.
[31] R. Li, C. Liu, J. Ma, Studies on the properties of graphene-oxide reinforced starch biocomposites, Carbohydr. Polym. 84 (2011) 631–637.
[32] Z. Xu, L. Zheng, S. Wen, L. Liu, Graphene oxide-supported zinc oxide nanoparticles for chloroprene rubber with improved crosslinking network and mechanical properties, Compos. Part A. Appl. S. (2019) 105492–105501.
[33] L.P. Lim, J.C. Juan, N.M. Huang, L.K. Goh, F.P. Leng, Y.Y. Loh, Enhanced tensile strength and thermal conductivity of natural rubber graphene composite properties via rubber-graphene interaction, Mater. Sci. Eng. B 246 (2019) 112–119.
[34] X.-W. Zhou, Y.-F. Zhu, J. Liang, Preparation and properties of powder styrene-butadiene rubber composites filled with carbon black and carbon nanotubes, Mater. Res. Bull. 42 (3) (2007) 456–464.
[35] F. Beck, J. Jiang, H. Krohn, Potential oscillations during galvanostatic over-oxidation of graphite in aqueous sulphuric acids, J. Electroana. Chem. 389 (1995) 161–165.
[36] N. Rattanasom, S. Prasertsri, K. Suchiva, Mechanical properties, thermal stability, gas permeability, and phase morphology in natural rubber/bromobutyl rubber blends, J. Appl. Polym. Sci. 113 (2009) 3985–3992.
[37] A.B. Suriani, M.D. Nurhafizah, A. Mohamed, A.K. Masrom, M.H. Mamat, M.F. Malek, M.K. Ahmad, M.S. Rosmi, M. Tanemura, Electrical enhancement of radiation-vulcanized natural rubber latex added with reduced graphene oxide additives for supercapacitor electrodes, J. Mater. Sci. 52 (2017) 6611–6622.
[38] A.B. Suriani, M.D. Nurhafizah, A. Mohamed, I. Zainol, A.K. Masrom, A facile one-step method for graphene oxide/natural rubber latex nanocomposite production for supercapacitor applications, Mater. Lett. 161 (2015) 665–668.